Applied Surface Science 256 (2010) 5006–5010

Contents lists available at ScienceDirect

Applied Surface Science

journal homepage: www.elsevier.com/locate/apsusc

Controllable synthesis of highly ordered Ag nanorod arrays by chemical deposition method

Jie Xu, Guo-an Cheng*, Rui-ting Zheng

Key Laboratory of Beam Technology and Material Modification of Ministry of Education, College of Nuclear Science and Technology, Beijing Normal University, Beijing 100875, PR China

ARTICLE INFO

Article history:
Received 30 November 2009
Received in revised form 8 March 2010
Accepted 8 March 2010
Available online 15 March 2010

Keywords:
Ag
Nanorod arrays
Chemical deposition
PAM template

ABSTRACT

Highly ordered Ag nanorod arrays were successfully fabricated using a simple chemical deposition method with the assistance of porous alumina membrane (PAM) template. The products were characterized by scanning electron microscopy (SEM), X-ray diffraction (XRD) and transmission electron microscopy (TEM). Ag^+ ions in the PAM nanochannels were reduced by acetaldehyde reagent and resulting in the formation of rod array structures. It is found that the diameter of the Ag nanorods is determined by the PAM template, and the length of the Ag nanorods is depended on the reaction temperature. The growth mechanism of the Ag nanorod arrays is investigated in the study.

1. Introduction

One-dimensional nanostructures have attracted extensive attention because of their unique physical and chemical properties [1,2] and the potential applications in nanoscale electronic, optical and mechanical devices [3–6]. Controllable growth of nanostructures is of great importance for the application of nanostructures [7,8]. Template assisted synthesis has proved to be a simple and versatile approach for preparing ordered nanowire, nanorod, nanoparticle and nanodot arrays in a wide range of materials [9–12]. Various nanostructured materials have been prepared by utilizing hard templates such as track-etched polycarbonate membranes [13], PAM templates [14–16] and soft templates such as polymers [17–18] and surfactants [19,20]. It has been found that the PAM is a relatively ideal template in producing controllable nanostructures because it has many desirable characteristics, such as hexagonal arranged pore arrays, uniform and parallel nanochannels, outstanding mechanical strength and highly thermal stability. In addition, the PAM thickness, pore diameter, inter-pore distance and porosity could be easily adjusted by controlling the experimental parameters, such as anodizing potential, oxidization duration and electrolyte concentration [21].

Ag exhibits high electrical and thermal conductivity. Recently, Ag is widely used as catalysts in the fabrication of nanoscale materials and act as electrocatalytical active surface in the fuel cells [22,23]. Nanoscaled Ag structures with well-controlled dimensions are always preferred for these applications. Several papers reported that the arranged Ag nanowires or nanorods could be synthesized by ultraviolet irradiation photoreduction method [24] or cyclic voltammetry electrodeposition process [25]. However, these methods need help of light or electrical source and make the experiment a little more complicated. In order to simplify the synthesizing process and achieve well-aligned Ag nanostructure, a chemical deposition method based on PAM template is developed. Wang et al. reported that evenly deposited Ag nanoparticles could be easily obtained with the assistance of PAM template via a typical silver mirror reaction process [26], large amount of Ag nanoparticles were reduced simultaneously and distribute randomly inside of PAM channels. However, we found that no string-like or rod-like Ag nanostructures could be synthesized by simply imitating the experimental parameters. Li et al. reported that the ordered Ag nanorods could be fabricated by a solvothermal and after-annealing approach [27]. The after-annealing process was applied to make the Ag particles coalesced into nanorods, but the additive heat treatment makes the nanorod surface rough, the nanorod discontinuous and the preparation more complicated. In this paper, we demonstrate a facile chemical deposition approach to fabricate large-scale Ag nanorod arrays. During the chemical deposition process, silver ammonia solution was firstly filled inside of PAM nanochannels. With the addition of reductant acetaldehyde, Ag^+ ions were reduced into nuclei, small Ag particles will slowly grow up in the channels and finally resulting in the formation of nanorod structures. Obviously, the diameter of the nanorods depends on the diameter of PAM channels, and the length of the Ag nanorods can be adjusted by

* Corresponding author. Tel.: +86 10 6220 5403; fax: +86 10 6220 5403.
E-mail address: gacheng@bnu.edu.cn (G.-a. Cheng).

0169-4332/$ – see front matter © 2010 Elsevier B.V. All rights reserved.
doi:10.1016/j.apsusc.2010.03.044

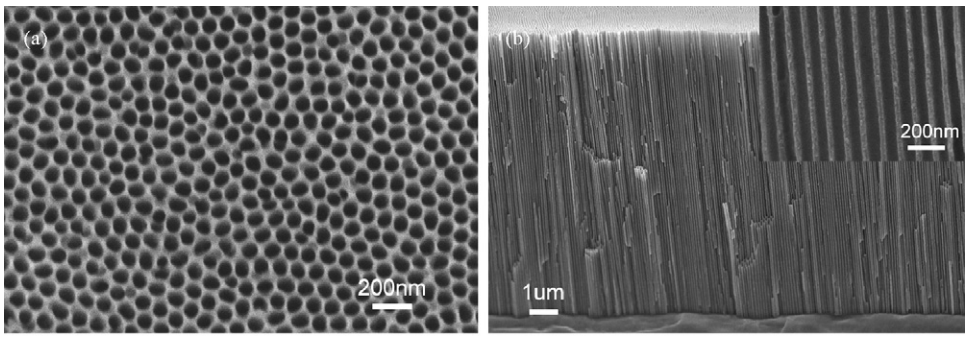

Fig. 1. FE-SEM images of ordered PAM templates fabricated after 5 min pore-widening process: (a) top view morphology and (b) cross-sectional view morphology, the inset in image (b) shows a magnified morphology of cross-sectional structure of PAMs.

controlling the reaction temperature in the experiment. The effect of temperature on the aspect ratio and morphology of nanorods was deeply studied.

2. Experimental

2.1. Preparation of template

The ordered hexagonal porous alumina templates were prepared via a two-step anodization process as described elsewhere [28]. High purity (99.999%) aluminum foils were annealed at 500 °C in a nitrogen atmosphere for 3 h to remove the inner mechanical stress and obtain the homogeneous condition for the later pore growth. Before anodization, the annealed aluminum foils were degreased in acetone and ethanol with the assistance of ultrasonic vibration. To obtain the smooth surface, the treated aluminum foils were then chemical polished in a mixture solution of H_3PO_4:H_2SO_4:HNO_3 = 5:4:1 (volume ratio) for 2 min. First anodization was carried out under a constant voltage of 40 V in 0.3 M oxalic acid solution at room temperature. After anodization for 30 min, the obtained oxide layer was stripped away by immersing in a mixture solution of H_3PO_4 acid (8 wt.%) and H_2CrO_4 acid (1.6 wt.%) at 45 °C for 30 min. The dissolution of the formed alumina leads to the patterned aluminum substrates, the regular hexagonal texture on the top of aluminum acts as a mask for the second anodization. Afterwards, the aluminum foil was re-anodized for 1 h under the same condition as the first step. The remaining aluminum was removed by dipping in a HCl (9 wt.%) and saturated $CuSO_4$ mixed solution for 2 min. Then the separated PAM was transferred to a Si substrate in the aqueous solution. Finally, the whole specimens were immersed in H_3PO_4 acid solution (8 wt.%) for 5 min at the temperature of 45 °C to remove the alumina barrier lay and achieve homogeneous nanochannels, this final chemical etching procedure was also defined as pore-widening process in the PAM fabrication.

2.2. Fabrication of Ag nanorod arrays

Ag nanorods were synthesized by a chemical deposition method. Firstly, the reaction beaker (10 ml) was degreased by washing with dilute NaOH solution (0.4 wt.%) for several times, this process also provides hydroxyls in the experiment to make the reaction solutions showing a weak alkaline property. Then $NH_3 \cdot H_2O$ solution (4 wt.%) was gradually dropped into $AgNO_3$ solution (3 wt.%) until the mixture become suspending status, gently stirring the solution to make the composites uniformly distributed, the pH value of the mixed solution was measured by a pH water-

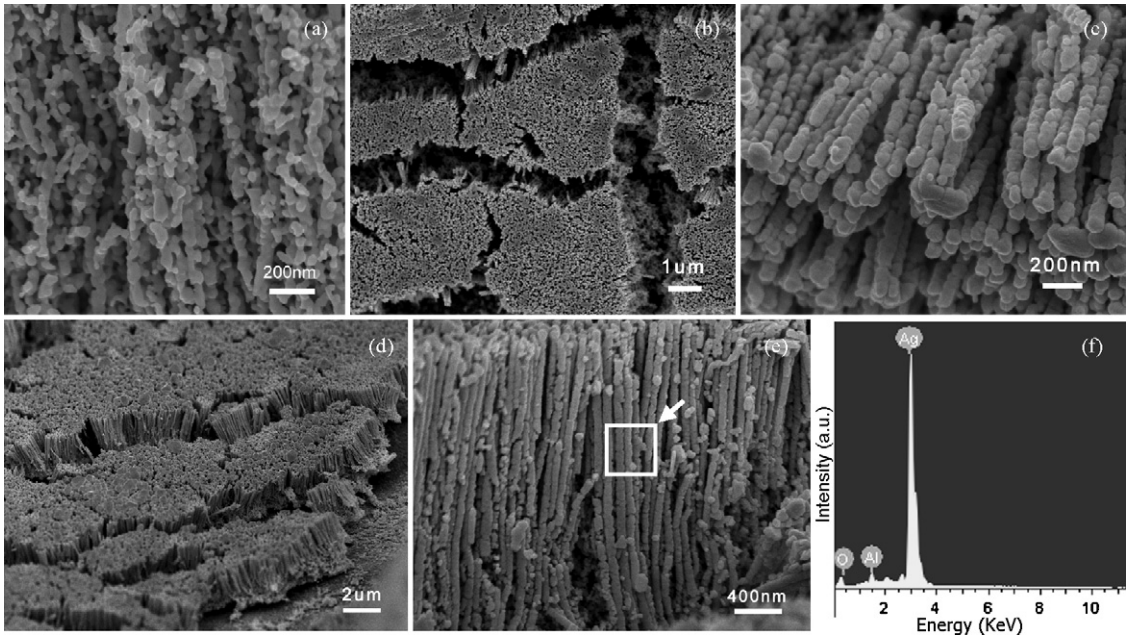

Fig. 2. FE-SEM images of the Ag nanostring/nanorod arrays synthesized under different temperatures: (a) 90 °C, (b) 40 °C, top view of Ag nanostring arrays, (c) 40 °C, cross-sectional view of Ag nanostring structure, (d) 0 °C, top view morphology of Ag nanorod arrays, (e) 0 °C, cross-sectional view morphology of Ag nanorods structure and (f) EDX compositional profile of the frame in image (e).

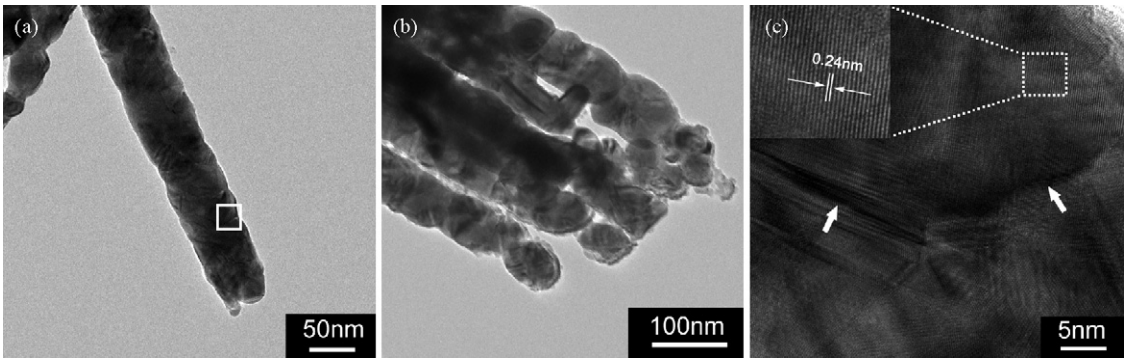

Fig. 3. TEM images of Ag nanorods: (a) a single Ag nanorod, (b) a bundle of Ag nanorods and (c) a HR-TEM image shows the interface between two Ag crystal grains.

proof meter (EXTECH, Exstik pH100), and it shows that the pH value of the silver ammonia solution was 8.5. Afterwards, the as-prepared PAM template was immersed into the mixed silver ammonia solution for 1 h, make sure the solution was fully dispersed in the PAM nanochannels, the immersing time should be carefully selected, since a short immersing time would affect the infiltration between solution and PAM template, while too long immersing time would result in the formation of Ag_3N in the solution. Finally, put the solution and PAM into a water bath vessel, which could adjust the solution temperature conveniently. At an appropriate temperature, add the reductant acetaldehyde (40 wt.%) into the solution slowly, Ag^+ ions and acetaldehyde will react fiercely in the PAM nanochannels and resulting in a large amount of nucleation centers, Ag nuclei would firstly form the small crystal particles and then grow up into Ag nanorods under the confinement of PAM nanochannels. Five temperatures (90 °C, 70 °C, 40 °C, 20 °C, 0 °C) were chosen to control the reaction rate of the reduction process.

2.3. Characterization

The morphologies of the products were observed by a field emission scanning electron microscope (FE-SEM) Hitach-S4800. Transmission electron microscope (TEM) observation was taken on JEM-2100F, with an accelerating voltage of 200 kV. X-ray diffraction (XRD) characterization was performed by a PANalytical/X'Pert-PRO-MPD diffractometer with Cu Kα radiation (wavelength 1.54056 Å). All the SEM images were further analysed by an Image-Proplus 5.0 software, which could get precise characteristic information directly from the electronic images. For the SEM and TEM observations, specimens were partially or completely immersed in 1 M NaOH solution to remove the residual PAM template.

3. Results and discussion

SEM images of PAM template prepared by two-step anodization and pore-widening process are shown in Fig. 1. After chemical etching in H_3PO_4 acid solution for 5 min, the PAM demonstrates perfectly hexagonal pore arrays. Fig. 1(a) indicates that the pore diameter is about 70 nm and the inter-pore distance is about 100 nm, so the pore density of the PAM sample is nearly 10^8 pores mm^{-2}. The cross-sectional view morphology of the PAM template shows that the nanochannels are highly ordered and parallel to each other, the thickness of the PAM is about 10 μm (Fig. 1(b)). The inset in Fig. 1(b) is a magnified cross-sectional image of the PAM, it further confirms that the nanochannels are perfectly arranged, they have straight and smooth inner surface as well as uniform diameters. Since the PAM morphology could be affected by the anodizing voltage and time, all the PAM samples used here were anodized under the same anodizing conditions.

Fig. 2 shows the FE-SEM images of Ag nanostructures under different preparing temperatures. All samples are partially immerged in 1 M NaOH solution to remove the PAM template. The product fabricated at temperature of 90 °C is shown in Fig. 2(a), it can be observed that there is no Ag nanorods formed. The PAM channels are filled with Ag nanoparticles, the particles adhere to each other and coalesce into a formicarium-like structure. Fig. 2(b) and (c) are the images of Ag nanostructures synthesized at 40 °C. As shown in Fig. 2(b), a large number of string-like Ag nanostructures are synthesized at this temperature. Fig. 2(c) is a cross-sectional view image of the Ag nanostring structures, the Ag nanostrings are parallel to each other, which is well consistent with the highly straight PAM pore channels. Although the morphology of nanostrings is much better than that fabricated at high temperatures (Fig. 2(a)), the outer surface of Ag nanostrings is still not perfect. Fig. 2(d) and (e) shows the top view and cross-sectional view of the rod-shape Ag nanostructures synthesized at 0 °C. Obviously, large-scale aligned Ag nanorod arrays can be found in Fig. 2(d). The Ag nanorods here are about 2 μm length and parallel to each other. As shown in Fig. 2(e), the morphology of Ag nanorods is greatly improved. The EDX spectrum of the white rectangle area in Fig. 2(e) is shown in Fig. 2(f). There are three peaks found, i.e., the strong Ag peak from the Ag nanorods, and the weak Al, O peaks due to the residual PAM fragments.

The individual Ag nanorod fabricated at 0 °C is further characterized by the TEM measurement after the PAM template was completely dissolved. A single Ag nanorod TEM image presented in Fig. 3(a) reveals that the diameter of the Ag nanorod is about 70 nm, which is in good agreement with the diameter of PAM nanochannels employed in the experiment (see e.g., Fig. 1(b)). A bundle of

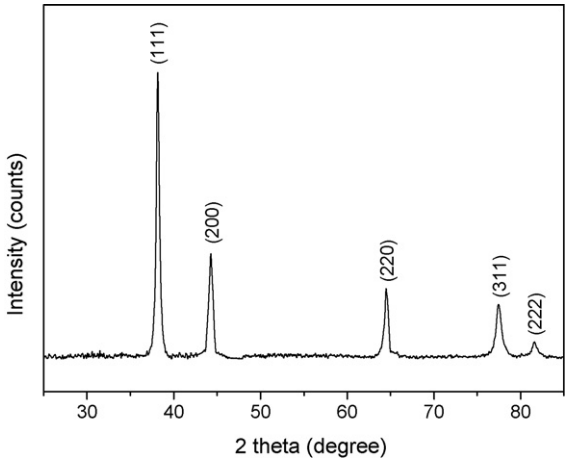

Fig. 4. XRD pattern of Ag nanorod arrays embedded in PAM template.

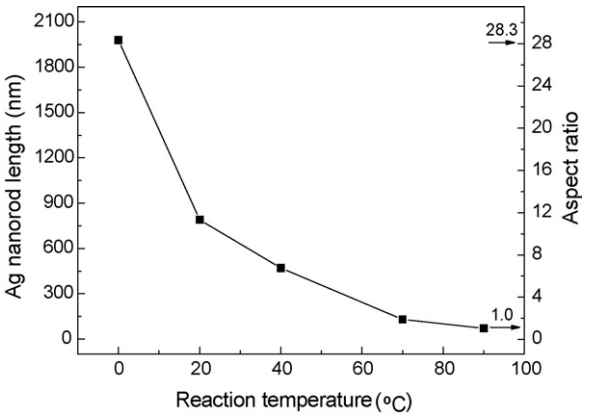

Fig. 5. The dependence of the Ag nanorods' length on the chemical reaction temperature.

Ag nanorods displayed in Fig. 3(b) indicate that the nanorods are well aligned even after totally removal of PAM template. A HR-TEM image corresponding to the white rectangle area in Fig. 3(a) is shown in Fig. 3(c). It can be seen that an apparent Ag grain boundary and some lattice defects such as dislocation and stacking faults displayed in the image (as the white arrow pointed out), which indicates the polycrystal nature of Ag nanorods. Due to the space restriction of PAM nanochannels, the outer surfaces of the Ag nanorods become round and smooth. The inset in Fig. 3(c) gives an enlarged image of the Ag particle, which reveals that the Ag particles are highly crystalline in nature and the lattice fringes are spaced 0.24 nm apart along the preferred growth orientation of [1 1 1] direction. It further supports the argument that the Ag nanorods are composed of Ag nanocrystals.

The XRD spectrum of the Ag nanorods embedded in the PAM is shown in Fig. 4. It can be seen that there are five peaks in the XRD spectra, which is corresponding to the (1 1 1), (2 0 0), (2 2 0), (3 1 1) and (2 2 2) planes of face-centered-cubic Ag (JCPDS card No. 65-2871), respectively. Due to the amorphous nature of PAM template, none Al_2O_3 reflection peaks are observed. It confirms that the regular and pure Ag nanorod arrays could be obtained by the simple chemical reduction process.

By comparing the Ag nanostructures synthesized under different temperature, we find that the diameter of Ag nanorods is determined by the parameters of as-prepared PAM templates, but the length of Ag nanorods has the relationship with preparing temperature. To investigate the temperature effects on the morphology of Ag nanorods, 5 different reaction temperatures are adopted. The dependence of the Ag nanorods' length on the chemical reaction temperature is shown in Fig. 5. Apparently, the nanorods' length decreased sharply with the increasing reduction temperature, i.e., the Ag nanorods have got a length nearly about 2 μm at 0 °C, but they only have several tens of nm under the temperature of 90 °C, which means the aspect ratio of nanorods could be adjusted from 28.3 to 1 in the experiment. The sharp decrease in Ag nanorods' length could be ascribed to the high chemical potential at a relatively high temperature, which makes silver nanoparticles grow faster. The chemical reactions may be expressed as:

$$AgNO_3 + 3NH_3{\cdot}H_2O \rightarrow Ag(NH_3)_2OH + NH_4NO_3 + 2H_2O \quad (1)$$

$$CH_3CHO + 2Ag(NH_3)_2OH \rightarrow CH_3COONH_4 + 2Ag\downarrow + 3NH_3 + H_2O \quad (2)$$

When the Ag^+ ions are reduced into Ag by acetaldehyde, they form a lot of nuclei. At a high temperature environment, high kinetic energy makes most of the Ag^+ ions in the solution are reduced and form a large number of big Ag nanoparticles simultaneously. These Ag particles discontinuously disperse in the channels and form a tousy structure (see e.g., Fig. 2(a)). At low temperature, only a part of Ag^+ ions are reduced into Ag nuclei at the beginning, latter

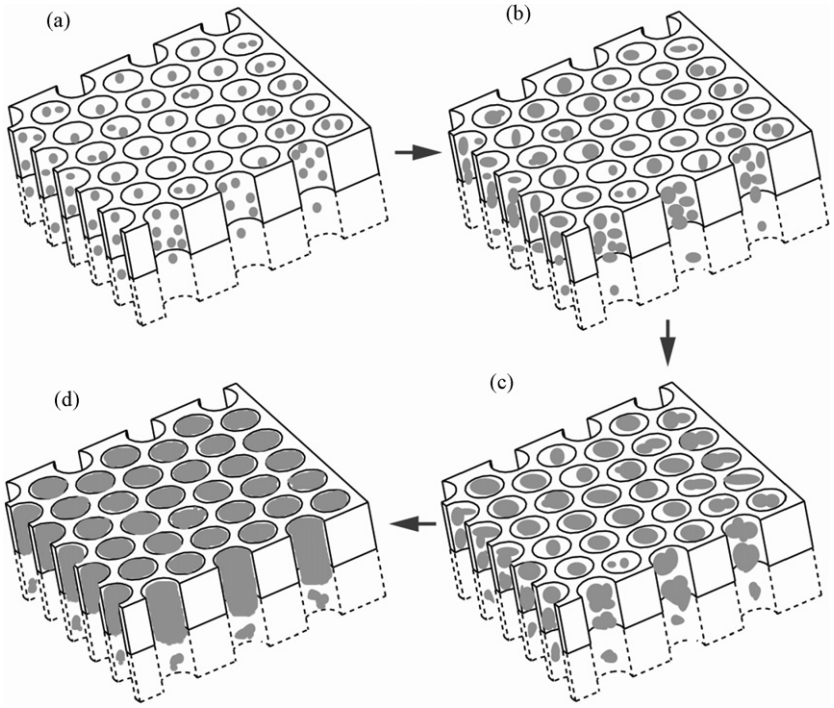

Fig. 6. Schematic diagrams of growth mechanism for the ordered Ag nanorod arrays: (a) Ag nuclei distribute evenly inside of PAM channels, (b) nuclei grow up into nanoparticles, (c) deep channels were blocked by Ag particles and (d) Ag nanorods were formed near the end of channels.

reduced Ag tend to absorb or grow on the surface of existing Ag particles to reduce surface energy, when the particles are grown up along the PAM channels, the straight and smooth Ag nanorods are synthesized.

The growth mechanism of the Ag nanorods in the PAM template channels is illustrated in Fig. 6. Firstly, the silver ammonia solution distributes evenly in the channels. With the addition of acetaldehyde, Ag^+ ions and reductant react with each other, resulting in the formation of a number of small Ag nuclei (Fig. 6(a)). Small Ag particles are formed and evenly distributed in the PAM channels (Fig. 6(b)), these Ag particles could provide low energy sites for the further nucleation and growth. With the increasing of chemical deposition time, more and more Ag particles deposit near the end of channels because of the sufficient Ag source is available at these places. This phenomenon will block the channels and seriously affect the Ag deposition inside the PAM channels (Fig. 6(c)). At last, regular Ag nanorods are formed near the end of the channels, but the internal parts of the channels are filled by discontinuous Ag particles (Fig. 6(d)). From above descriptions, it could be realized that the chemical reaction rate will affect the Ag deposition inside the PAM channels. By decreasing the reaction temperature, chemical reactants could get enough time to diffuse deeply inside the channels before these channels are blocked, it means the Ag nanorods will get more Ag source to grow up, and the longer Ag nanorods could be obtained.

4. Conclusions

In summary, a simple method of chemical deposition silver into the nanochannels of PAM template is presented. Large-scale ordered Ag nanostrings were successfully synthesized. The dimension and the morphology of Ag nanostrings depend on the PAM template and deposition process. Ag nanorods with the uniform diameter and controllable aspect ratio could be fabricated by optimizing the reaction temperature. The growth of the Ag nanorods is affected by the chemical deposition rate of Ag nanoparticles inside the PAM channels.

Acknowledgements

This work was supported by the National Basic Research Program of China (No: 2010CB832905), and partially by the National Natural Science Foundation of China (grant No. 10575011) and the Key Project of Science and Technology of Education of China (grant No. 108124).

References

[1] C.M. Lieber, Solid. State Commun. 107 (1998) 607.
[2] J. Hu, T.W. Odom, C.M. Lieber, Acc. Chem. Res. 32 (1999) 435.
[3] X.F. Duan, Y. Huang, Y. Cui, J. Wang, C.M. Lieber, Nature 409 (2001) 66.
[4] Y.N. Xia, P.D. Yang, Y.G. Sun, Y.Y. Wu, B. Mayers, B. Gates, Y.D. Yin, F. Kim, H.Q. Yan, Adv. Mater. 15 (2003) 353.
[5] M.H. Huang, S. Mao, H. Feick, H. Yan, Y. Wu, H. Kind, E. Weber, R. Russo, P. Yang, Science 292 (2001) 1897.
[6] C.Z. Li, H.X. He, A. Bogozi, J.S. Bunch, N.J. Tao, Appl. Phys. Lett. 76 (2000) 1333.
[7] M. Hu, J. Chen, Z.Y. Li, L. Au, G.V. Hartland, X. Li, M. Marquez, Y. Xia, Chem. Soc. Rev. 35 (2006) 1084.
[8] Z.L. Wang, J. Phys.: Condens. Matter 16 (2004) 829.
[9] T.M. Whitney, J.S. Jiang, P.C. Searson, C.L. Chien, Science 261 (1993) 1316.
[10] T.L. Wade, J.E. Wegrowe, Eur. Phys. J. Appl. Phys. 29 (2005) 3.
[11] M.S. Bakshi, P. Sharma, T.S. Banipal, Mater. Lett. 61 (2007) 5004.
[12] S.K. Park, J.S. Noh, W.B. Chin, D.D. Sung, Curr. Appl. Phys. 7 (2007) 180.
[13] S. Demoustier-Champagne, M. Delvaux, Mat. Sci. Eng. C 15 (2001) 269.
[14] G.Q. Ding, W.Z. Shen, M.J. Zheng, D.H. Fan, Appl. Phys. Lett. 88 (2006) 103106.
[15] X.W. Wang, G.T. Fei, X.J. Xu, Z. Jin, L.D. Zhang, J. Phys. Chem. B 109 (2005) 24326.
[16] C.R. Martin, Science 266 (1994) 1961.
[17] S. Sumikura, S. Mori, S. Shimizu, H. Usami, E. Suzuki, J. Photochem. Photobiol. A 199 (2008) 1.
[18] D. Wan, H. Pu, Mater. Lett. 61 (2007) 3404.
[19] T. Wang, L. Dai, Colloid Surface. A 209 (2002) 65.
[20] M.S. Bakshi, P. Sharma, T.S. Banipal, Matter. Lett. 61 (2007) 5004.
[21] A. Belwalkar, E. Grasing, W.V. Geertruyden, Z. Huang, W.Z. Misiolek, J. Membr. Sci. 319 (2008) 192.
[22] M.A. Kostowskyj, R.J. Gilliam, D.W. Kirk, S.J. Thorpe, Int. J. Hydrogen Energy 33 (2008) 5773.
[23] S. Rather, M. Naik, S.W. Hwang, A.R. Kim, K.S. Nahm, J. Alloy. Compd. 475 (2009) L17.
[24] Y. Zhou, S.H. Yu, C.Y. Wang, X.G. Li, Y.R. Zhu, Z.Y. Chen, Adv. Mater. 11 (1999) 850.
[25] X. Sun, F. Xu, Z. Li, W. Zhang, Mater. Chem. Phys. 90 (2005) 69.
[26] G. Wang, C. Shi, N. Zhao, X. Du, Mater. Lett. 61 (2007) 3795.
[27] X. Li, D. Wang, L. Tang, K. Dong, Y. Wu, P. Yang, P. Zhang, Appl. Surf. Sci. 255 (2009) 7529.
[28] H. Masuda, K. Fukuda, Science 268 (1995) 1466.